HHS Public Access

Author manuscript

J Am Chem Soc. Author manuscript; available in PMC 2017 September 28.

Published in final edited form as:

J Am Chem Soc. 2016 September 28; 138(38): 12527–12533. doi:10.1021/jacs.6b06823.

Identification of Mechanism-Based Inactivation in P450-Catalyzed Cyclopropanation Facilitates Engineering of Improved Enzymes

Hans Renata[a,‡,†], **Russell D. Lewis**[a,‡], **Michael J. Sweredoski**[b], **Annie Moradian**[b], **Sonja Hess**[b], **Z. Jane Wang**[a], and **Frances H. Arnold**[a,*]

[a]Division of Chemistry and Chemical Engineering, MC 210-41, California Institute of Technology, 1200 E California Blvd, Pasadena, CA 91125, United States

[b]Proteome Exploration Laboratory, Division of Biology and Biological Engineering, Beckman Institute, MC 139-74, California Institute of Technology, 1200 E California Blvd, Pasadena, CA 91125, United States

Abstract

Following the recent discovery that heme proteins can catalyze the cyclopropanation of styrenyl olefins with high efficiency and selectivity, interest in developing new enzymes for a variety of non-natural carbene transfer reactions has burgeoned. The fact that diazo compounds and other carbene precursors are known mechanism-based inhibitors of P450s, however, led us to investigate if they also interfere with this new enzyme function. We present evidence for two inactivation pathways that are operative during cytochrome P450-catalyzed cyclopropanation. Using a combination of UV-Vis, mass spectrometry, and proteomic analyses, we show that the heme cofactor and several nucleophilic side chains undergo covalent modification by ethyl diazoacetate (EDA). Substitution of two of the affected residues with less-nucleophilic amino acids led to a more than two-fold improvement in cyclopropanation performance (total TTN). Elucidating the inactivation pathways of heme protein-based carbene transfer catalysts should aid in the optimization of this new biocatalytic function.

Graphical abstract

[*]**Corresponding Author**. frances@cheme.caltech.edu.

[†]**Present Addresses**

Department of Chemistry, The Scripps Research Institute, 130 Scripps Way, Jupiter, FL 33458.

[‡]H.R and R.D.L. contributed equally.

ASSOCIATED CONTENT

Supporting Information

The Supporting Information is available free of charge on the ACS Publications website.

Supplementary figures, methods, and general procedure (PDF)

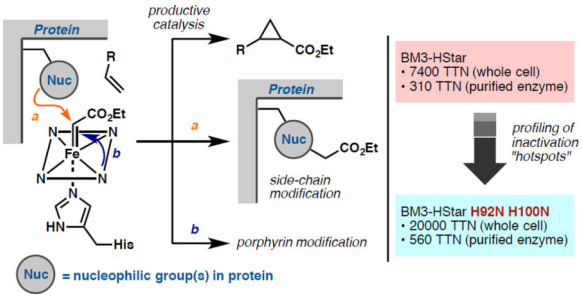

Introduction

Over the past few years, we[1] and others[2] have reported that engineered P450 enzymes and other heme proteins can catalyze non-natural carbene transfer reactions, *e.g.* olefin cyclopropanation (Figure 1A), with high efficiency and selectivity. The proposed catalytic cycle initiates by reduction of the ferric enzyme to the ferrous counterpart which then reacts with a diazo molecule to form an iron carbenoid intermediate. Transfer of the carbene fragment to a second substrate forms product and regenerates the active ferrous enzyme. Even though the formation of iron carbenoids in P450s has been described in the literature,[3–6] our report in 2013[1a] was the first example of their use in productive enzymatic catalysis. Indeed, P450s were reported to undergo suicide inactivation in the presence of halothane[3] and CCl_4[4], whereby a putative iron carbenoid led to covalent modification of the enzymes and irreversible loss of activity. Similarly, the decomposition of 3-[[2-(2,4,6-trimethylphenyl)thio]ethyl]-4-methylsydnone by rat liver P450 was proposed to proceed via an iron carbenoid intermediate that reacted with the heme cofactor to form *N*-vinylprotoporphyrin IX.[5]

Because understanding inactivation pathways can facilitate development of more stable and efficient enzymes,[7] we investigated whether the P450-derived ‘carbene transferase’ is inactivated by mechanisms similar to the suicide inactivation induced by iron carbenoid formation in native P450s. Covalent modification of the heme cofactor or protein side chains by the reactive carbenoid intermediate (Figure 1B) would compete with product formation and ultimately destroy the catalyst. Our goal is to understand the mechanism of inactivation and delay or circumvent it by engineering the protein sequence.

Results

EDA-Induced Inactivation of a P450-Based Cyclopropanation Enzyme

We previously discovered that substitution of the proximal cysteine ligand with histidine in cytochrome P450-BM3 led to a highly active cyclopropanation catalyst.[1c] This finding enabled the engineering of a histidine-ligated P450 (BM3-HStar: P450-BM3 V78M L181V T268A C400H L437W) that catalyzes the cyclopropanation of phenylacrylamide **1** in a highly stereoselective fashion en route to the synthesis of levomilnacipran, an FDA-approved antidepressant. During efforts to scale up the *E. coli* whole-cell catalyst expressing BM3-HStar, we observed a substantial decrease in the yield and selectivity of the reaction at high substrate concentrations. While the reaction provided high yield (92%) and selectivity

(92% ee) at 10 mM substrate **1** concentration (20 mM EDA), we found that it afforded only 28% yield and 50% ee at 50 mM loading (100 mM EDA) (Scheme 1) and was completely non-stereoselective at 150 mM (300 mM) loading. This observation led us to believe that an inactivation pathway was interfering with selectivity and preventing further conversion at higher concentrations of olefin and EDA.

We chose to investigate inactivation of the isolated BM3-HStar enzyme in order to avoid possible complications from cellular components. From control experiments, we noted that purified enzyme[8] that was pre-incubated with EDA in the absence of $Na_2S_2O_4$ retained virtually all of its catalytic activity, whereas pre-incubation with EDA and reductant led to rapid inactivation (Figure S1). The fact that inactivation requires reductant suggests a mechanism that involves more than simple EDA binding and instead implies a pathway that generates a reactive species through reaction of the ferrous heme with the diazo compound, consistent with the observation that P450-catalyzed cyclopropanation proceeds from the ferrous state.[1,9] Thus, we suspected a mechanism-based inactivation pathway whereby the reactive iron carbenoid species undergoes undesired side reactions with the enzyme. In the presence of the olefin substrate these side reactions could compete with productive cyclopropanation, eventually leading to complete catalyst inactivation.

Extent of Heme Cofactor Modification

Previous reports of mechanism-based P450 inactivation indicate that carbene precursors can lead to covalent modification of the heme prosthetic group or protein side chain(s).[3–6,10,11,12] In particular, Ortiz de Montellano and co-workers observed porphyrin modification in the reaction of P450 and model Fe-porphyrin complexes with 3-[[2-(2,4,6-trimethylphenyl)thio]ethyl]-4-methylsydnone[5] or diazoacetophenone[11] and proposed an intramolecular carbene insertion reaction to account for their observations. To investigate whether an analogous pathway is operative in our system, we analyzed the porphyrins from the reaction of EDA and **1** using purified BM3-HStar and quenched after 15 s and 1 min. After extraction from the reaction mixture, the crude organics were analyzed by liquid chromatography-mass spectrometry (LC-MS) using detection at 330 nm to minimize background signal. In agreement with the observed dependence of enzyme inactivation on presence of the reductant, extracts from reaction mixture that did not contain $Na_2S_2O_4$ yielded a single species with a mass spectrum and retention time that correspond to unmodified Fe-protoporphyrin IX (Fe-PPIX) cofactor, as determined by LC-MS analysis of authentic standard (Figure 2). However, the crude extracts obtained after 15 s of reaction of **1** and EDA using reduced BM3-HStar showed diminished signal for Fe-PPIX and the presence of additional species. Strikingly, no unmodified Fe-PPIX remained in the reaction mixture quenched after 1 min. Similar analyses performed with other heme protein-based carbene transfer catalysts, myoglobin (Mb) mutant H64V V68A[2b] and a Ser-ligated P450-BM3,[1b] also revealed loss of Fe-PPIX (See Supporting Information, Figure S2 and S3).

Thin-layer chromatography (TLC) analysis of the reaction mixture indicated the presence of a new red-fluorescent band, which was subsequently purified by preparative TLC and analyzed by UV-Vis spectroscopy and mass spectrometry. Absorption spectra obtained for the isolated porphyrin species showed that it is distinct from PPIX, both as the free

porphyrin (Figure S4) and as the Zn complex (Figure 3). The absorption spectrum of the modified porphyrin after complexation with Zn^{2+} yielded a Soret peak at 430 nm with a slight shoulder, which is a characteristic feature of *N*-alkylprotoporphyrin derivatives.[5] Furthermore, the mass spectrum of the isolated porphyrin exhibited two major peaks with *m/z* of 735.3374 and 821.3753, corresponding to loss of Fe^{3+} and addition of two and three ethyl acetylidene fragments ($C_4H_6O_2$, *m/z* = 86.1 Da) to the heme cofactor, respectively. These lines of evidence, together with previous literature on P450 cofactor modification,[5,11,13] point to *N*-alkylation of the cofactor during the cyclopropanation reaction.

Evidence for Modification of Protein Side Chains and Resulting Structural Changes

Given the precedent of protein side chain alkylation during oxidation of acetylenic compounds,[10] we investigated whether a similar phenomenon occurs during the enzyme-catalyzed cyclopropanation reaction. To this end, cyclopropanation was performed with purified BM3-HStar, quenched after 15 s, and the crude reaction mixture was submitted to mass spectrometry (MS) analysis. Extreme heterogeneity of the enzyme could already be observed (Figure S5). Deconvolution of the mass spectrum afforded multiple species with molecular weights that correspond to integer number additions of the carbene fragment (86 Da). Under the denaturing conditions used for MS analysis, the heme cofactor is extruded from the protein. Thus, any observed mass difference in the spectra can be attributed solely to modification of the polypeptide chain.

Circular dichroism (CD) spectroscopy of EDA-treated enzyme also showed changes relative to unreacted enzyme in the far-UV region (Figure 4). We noted reduced molar ellipticity at 222 nm, which suggests decreased α-helical content and increased random coil content of the protein. Taking into account both the MS and CD spectral observations, we propose a model wherein EDA modifies the cofactor and multiple protein side chains, leading to disruption of secondary structures and partial unfolding. Comparison of these data and LC-MS observation of cofactor modification suggest that the side chain and porphyrin alkylations happen on similar time scales, although we cannot determine the exact order of events.

Identification of Modified Residues

To identify the residues that are modified during the initial stages of the reaction, protein from the crude cyclopropanation reaction mixture after 5 s was analyzed by trypsin digestion followed by tandem LC-MS/MS analysis. From this analysis (Figure 5), we observed modifications (underlined residues indicate the site of modification) on peptide fragments EA<u>C</u>DESRFDK (residues 60–69), NL<u>S</u>QAL<u>K</u>FM<u>R</u> (residues 70–79), DFAGDGLFTSWT<u>H</u>EK (residues 80–94), and A<u>H</u>NILLPSFSQQAMK (residues 99–113). Modifications were addition of a $C_4H_6O_2$ fragment (86.1 Da), corresponding to the ethyl acetylidene moiety, onto residues C62, S72, K76, R79, H92, and H100. We also observed modification of residue K69 on fragment FD<u>K</u>NLSQALK (residues 67–76) in samples taken at later time points. Control experiments with CO-treated enzyme (inactive for cyclopropanation) revealed much-diminished signals for modified peptides during the proteomic analysis, again suggesting that the iron carbenoid generated from the ferrous

heme is responsible for the modifications. That the affected residues are all nucleophilic in nature is consistent with the proposed electrophilic character of the carbenoid species.[14] Modifications presumably occur by way of O–, N–, and S– alkylation by the carbene fragment.

In the absence of a crystal structure for His-ligated P450-BM3, the crystal structure of wild-type (WT) BM3 (PDB ID: 2IJ2) was used to map the locations of these residues relative to the heme cofactor (Figure 6). To our surprise, other than K69, which makes a polar contact with the propionate moiety of the heme cofactor, all the alkylated residues are more than 10 Å away from the iron center. One possible explanation is that the Hstar active site is devoid of nucleophilic residues, and that all likely alkylation targets are distant. It is worth noting, however, that residues S72, K76, R79 are situated in the B'-helix and H92 is in the B'/C loop. The B'-helix has been proposed as an important recognition site[15] that controls substrate specificity in P450s. It has also been shown crystallographically that a single mutation (F81L) in this region can effect its collapse towards the active site.[16] Moreover, our recent report[17] on the X-ray crystal structure of His-ligated CYP119 shows notable rearrangements in the protein to compensate for non-native ligation, including unresolved portions in the B'- and F-helices and increased disorder in the C-helix. If similar rearrangements occur upon mutation of the axial residue from Cys to His in P450-BM3, it is possible that the region where S72, K76, R79, and H92 reside undergoes large-scale movements that bring them closer to the active site. Furthermore, the P450s possess remarkable structural plasticity,[18] and iron carbenoid formation could also induce structural and dynamic changes that bring this region in closer contact. In addition to the possibility that structural plasticity accounts for the distance of the alkylated sites from the iron center, recent computational studies by Khade *et al.*[14a] also invoked a dative bond from the carbene moiety to Fe, which could implicate a diffusible carbene species in the active site and might account for the observed alkylation pattern.

The remaining three alkylated residues also deserve mention, as we surmise that they would play vital roles in maintaining the folded structure of P450-BM3. As previously noted, K69 is involved in a polar contact with the heme prosthetic group (Figure S7). H100 is implicated in a hydrogen bonding interaction with the FMN domain of the fused reductase partner and is conserved as a basic amino acid residue in P450s.[19] Mutation of C62 in P450-BM3 has been reported to lower thermostability.[20] Thus, modifications of these residues could result in disruption of key interactions and loss of structural integrity.

Site-directed Mutagenesis of Modified Residues Improves Catalyst Performance

The observations outlined above indicate that these modifications have deleterious effects on the secondary structure of the enzyme and the efficiency of the cyclopropanation reaction. We hypothesized that even though BM3-HStar will eventually be inactivated through modification of the heme prosthetic group, mutations of the alkylated residues to attenuate their nucleophilicity might better preserve structure and function during the reaction and, ultimately, improve carbene transfer efficiency to the substrate (measureable in terms of total turnover number to product). We therefore created seven single variants of BM3-HStar in which the alkylated residues were replaced with their non-nucleophilic isosteres. This design

entails mutation of His to Asn (mutations H92N and H100N), Arg to Gln (mutation R79Q), Cys and Ser to Ala (mutations C62A and S72A), and Lys to Arg (mutations K69R and K76R). The seven variants were first tested for cyclopropanation activity in cell lysate. Three of the variants, C62A, K69R, and K76R, were poorly expressed and not studied further. Two of the variants, H92N and H100N, gave improved total turnover numbers (1.2- and 1.4-fold improvement, respectively) for the formation of **2**, while the remaining two failed to yield any improvements. Following this observation, we characterized the performance of the purified H92N and H100N variants and were pleased to observe similar enhancements in cyclopropanation activity. While purified BM3-HStar showed only modest conversion and poor selectivity, variants H92N and H100N in purified form gave much improved reaction yields and selectivities for cyclopropanation of **1** (Figure 7). Moreover, these two mutations could be recombined in a double variant H92N H100N that, as purified enzyme, afforded up to 560 TTN (0.1% enzyme loading, 1.8-fold improvement over BM3-HStar) and 98:2 dr and 87% ee; selectivity numbers that are very close to those previously observed in reactions with whole cells expressing BM3-HStar (Scheme 1).

Next, we evaluated the performance of the new variants in whole-cell reactions, as the enzymes have hitherto provided superior performance when used as whole-cell catalysts. Gratifyingly, the improvement was even more significant (Figure 8). In particular, variant H92N H100N gave more than 20,000 TTN in the production of **2** (2.7-fold improvement over BM3-HStar), while maintaining the excellent diastereo- and enantioselectivity of the parent catalyst. Variants H92N, H100N, and H92N H100N express at similar levels to parent enzyme BM3-HStar (0.20–0.25 μM at OD_{600} = 10, see Supporting Information for determination of protein concentration in whole-cell suspension). Thus the observed increase in TTN translates to similar improvements in product/dry cell weight.

Finally, the improvement in activity imparted by mutations H92N and H100N could be generalized to other carbene transfer reactions, including styrene cyclopropanation and carbenoid insertion into the N–H bond of aniline (Figure S8). Under whole-cell reaction conditions, HStar H92N H100N yielded 55% and 30% increases in styrene cyclopropanation and aniline N–H insertion activities over unmutated BM3-HStar.

Characterization of BM3-HStar H92N H100N

Comparing the kinetics of formation of **2** with BM3-HStar and HStar H92N H100N under whole-cell reaction conditions at 10 mM substrate concentrations and *ca.* 0.2 μM enzyme concentration shows that the engineered variant supports faster product formation, but both rates decrease after ~ 30 min (Figure S9, Supporting Information). We performed similar inactivation analyses on BM3-HStar H92N H100N to find out whether the inactivation mechanism had changed. We noted changes in the CD spectral features upon treatment of ferrous BM3-HStar H92N H100N with EDA, similar to BM3-HStar (Figure S10, Supporting Information). In addition, bottom-up proteomic analyses indicated that residues K69, S72, K76, S89, K97, S304, and K306 of BM3-HStar H92N H100N were alkylated during the initial stages of this reaction, but no modification occurred at N92 or N100 (Figure S11). Of these, only K69, S72, and K76 were observed to undergo modification in the parent enzyme BM3-HStar. Lastly, LC-MS analysis of purified BM3-HStar H92N

H100N after cyclopropanation showed that the porphyrin cofactor underwent identical alkylative modifications as in BM3-HStar.

Discussion

Various reports of irreversible inhibition of P450s by carbene precursors led us to investigate whether such pathways compete with productive catalysis in engineered “carbene transferases” derived from heme-containing proteins. This new enzyme activity involves a reactive intermediate that can damage the cofactor and protein if the carbene is not efficiently transferred to the substrate. Mutations to the protein sequence could assist productive catalysis, either by promoting productive transfer through improved binding and orientation of the substrate or by disfavoring non-productive transfer to the protein itself. Evolution finds both types of solutions by molding the protein active site and dynamics to promote productive catalysis, even when highly reactive species are generated during the catalytic cycle. Native P450 reactions that go through Compound I provide an excellent example of how an enzyme can generate a highly reactive species and direct it (most of the time) to a substrate. In contrast to P450-catalyzed monooxygenations, however, the newly-developed carbene transfer activities of heme proteins have not yet been highly tuned by evolution. We are starting to investigate opportunities for enhancing this non-natural activity by directed evolution[1] and rational engineering based on understanding some of the failure modes.

We found that the heme cofactor and several nucleophilic residues are modified by transfer of the reactive carbene to the enzyme rather than the olefin substrate during cyclopropanation of phenylacrylamide with EDA. Up to three additions of ethyl acetylidene fragment on the porphyrin were observed, and spectroscopic analysis of the modified porphyrin species suggests the formation of *N*-alkylporphyrin products. Presumably, this modification also interferes with metal binding, leading to the expulsion of Fe^{3+} as seen in the mass spectrum. These results suggest erosion of the active heme species, eventually leading to complete loss of the cofactor and catalytic function. Similar cofactor loss during reactions with other heme protein-based catalysts (myoglobin and a Ser-ligated P450) suggests that this off-cycle reaction is an inherent feature of porphyrin-based protein catalysts of carbene transfer reactions.

We also obtained evidence that carbenoid formation can result in the modification of protein side chains and disruption of BM3-HStar secondary structure. The observation of multiply modified species in the proteomic analyses implies that BM3-HStar is still capable of reacting with EDA even after initial modification. However, the iron carbenoid species might possess increasingly diminished reactivity and/or selectivity for productive cyclopropane formation due to the cumulative effects of protein structural modifications, accounting for the observed erosion in selectivity of BM3-HStar at high substrate concentrations and during pre-incubation with EDA.

We reasoned that reducing the nucleophilicity of some of the modified residues could reduce protein damage and possibly lead to better secondary structure preservation during the reaction and less inactivation. We identified two beneficial mutations, H92N and H100N,

that improve carbene transfer activity and selectivity. That BM3-HStar double mutant H92N H100N performed better in other types of carbene transfer reactions—styrene cyclopropanation and N–H insertion—indicates that the improvements are general rather than specific to substrate **1**. A possible explanation for the effects of the mutations is that the reaction ensemble contains more active form of the enzyme. BM3-HStar H92N H100N, however, still undergoes irreversible inactivation: even though the mutations avert potentially deleterious modification at residues 92 and 100, the reactive iron carbenoid species nonetheless inflicts alkylative damage on the porphyrin and other nucleophilic residues, including several that did not appear to be alkylated in BM3-HStar. It remains to be seen whether further protein engineering, including directed evolution, can generate an enzyme that better directs the reactive carbenoid intermediate to reaction with the second substrate, as the native cytochrome P450 does with its highly reactive oxygen intermediates during the native reaction.

Our results indicate that EDA-induced inactivation is operative in reactions with purified enzyme and whole-cell catalyst. Yet, the relative rates of inactivation are strikingly different, with purified enzyme suffering much more rapid inactivation as well as inferior initial activity and selectivity. The origins of this difference are not yet clear, but several possible explanations can be put forth. One is that cellular components contribute to higher enzyme stability through the protective effects of, for example, molecular chaperones[21], macromolecular crowding[22], or even cytoplasmic molecules acting as sacrificial carbene acceptors. His-ligated heme proteins such as the globins are also known to undergo heme exchange and dissociation;[23] heme exchange in the cell could replenish the cofactor and prolong the lifetime of the catalyst. Finally, it is possible that the rate of inactivation depends on the protein fold or family, and future studies will investigate the robustness of different heme protein scaffolds for carbene transfer reactions.

Conclusions

Exploiting the ability of proteins to evolve and adapt to new challenges, our laboratory has developed variants of P450-BM3 as platforms for non-natural reactions with xenobiotic diazo compounds. However, introduction of xenobiotic reagents to natural enzymes can lead to undesired repercussions such as inactivation.[7] We have provided clear evidence for mechanism-based inactivation of a His-ligated P450-BM3 variant by ethyl diazoacetate that results in the modification of the heme prosthetic group and several protein side chains, which degrades enzyme performance and causes irreversible activity loss. Site-directed mutagenesis of some of the affected residues to amino acids that are less easily modified created superior variants with improved cyclopropanation activity as both purified enzymes and whole-cell catalysts.

An alternate approach to optimization of enzymes for non-natural reactions would be to accumulate beneficial mutations by random mutagenesis and high throughput screening (classical directed evolution). However, screening can be challenging for some reactions, especially when high enantioselectivity is desired. For this reason, directed evolution to date has focused on active site residues defined for the wild type enzyme. However, this approach places little consideration on the potential incompatibility of the xenobiotic reagents with

biological systems, which could render the enzyme susceptible to harmful off-cycle reaction(s). Tracing the catalyst's fate during the reaction enables the identification of such inactivation "hotspots", and allows for the discovery of beneficial mutations at more distant residues. Echoing a recent report on mitigation of substrate inhibition in a DERA enzyme,[7c] our results demonstrate the merits of mechanistic analyses in improving the overall activity of enzymes for biotechnological applications, especially ones that are employed in non-native environments. Given the growing interest in the development of biocatalytic carbene transfer reactions, we expect that the inactivation profiling and rational engineering approach we outline here will be generally useful for creating "carbene transferases" with improved lifetimes and tolerance to reaction conditions for synthetic applications.

Supplementary Material

Refer to Web version on PubMed Central for supplementary material.

Acknowledgments

The authors thank Dr. Andrew R. Buller, Dr. Christopher K. Prier, Dr. David K. Romney, and Dr. Sabine Brinkmann-Chen for helpful comments on the manuscript. We thank the staff of the Proteome Exploration Laboratory at Caltech, especially Roxana Eggleston-Rangel, for assistance with the proteomic analyses, Dr. Scott Virgil and the Caltech Center for Catalysis and Chemical Synthesis (3CS) for assistance with SFC and HRMS analyses, and the Beckman Institute Laser Resource Center (BILRC) at Caltech for use of their CD spectrometer. This work was supported by the Gordon and Betty Moore Foundation through grant GBMF2809 to the Caltech Programmable Molecular Technology Initiative, and the National Science Foundation, Office of Chemical, Bioengineering, Environmental and Transport Systems SusChEM Initiative (grant CBET-1403077). The Proteome Exploration Laboratory is supported by the Gordon and Betty Moore Foundation through grant GBMF775, and the Beckman Institute. R.D.L. is supported by NIH/NRSA training grant (5 T32 GM07616).

REFERENCES

1. a) Coelho PS, Brustad EM, Kannan A, Arnold FH. Science. 2013; 339:307–310. [PubMed: 23258409] b) Coelho PS, Wang ZJ, Ener ME, Baril SA, Kannan A, Arnold FH, Brustad EM. Nat. Chem. Biol. 2013; 9:485–487. [PubMed: 23792734] c) Wang ZJ, Renata H, Peck NE, Farwell CC, Coelho PS, Arnold FH. Angew. Chem. Int. Ed. 2014; 53:6810–6813.d) Heel T, McIntosh JA, Dodani SC, Meyerowitz JT, Arnold FH. Chem Bio Chem. 2014; 15:2556–2562.
2. a) Sreenilayam G, Fasan R. Chem. Commun. 2015; 15:1532–1534.b) Bordeaux M, Tyagi V, Fasan R. Angew. Chem. Int. Ed. 2015; 54:1744–1748.c) Tyagi V, Bonn RB, Fasan R. Chem. Sci. 2015; 6:2488–2494. [PubMed: 26101581] d) Gober JG, Rydeen AE, Gibson-O'Grady EJ, Leuthaeuser JB, Fetrow JS, Brustad EM. Chem Bio Chem. 2015; 17:394–397.
3. a) Mansuy D, Nastainczyk W, Ullrich V. Arch. Pharmacol. 1974; 285:315–324.b) Nastainczyk W, Ullrich V, Sies H. Biochem. Pharmacol. 1978; 27:387–392. [PubMed: 629799] c) Krieter PA, Van Dyke RA. Chem-Biol. Interact. 1983; 44:219–235. [PubMed: 6872091] d) Manno M, Cazzaro S, Rezzadore M. Arch. Toxicol. 1991; 65:191–198. [PubMed: 2053846]
4. a) Wolf CR, Mansuy D, Nastainczyk W, Deutschmann G, Ullrich V. Molec. Pharmacol. 1977; 13:698–705. [PubMed: 18662] b) Manno M, Reed C, King LJ, De Matteis F. Arch. Toxicol. Suppl. 1988; 12:315–317.c) Manno M, De Matteis F, King LJ. Biochem. Pharmacol. 1988; 37:1981–1990. [PubMed: 3377806]
5. Ortiz de Montellano PR, Grab LA. J. Am. Chem. Soc. 1986; 108:5584–5589.
6. Groves JT, Avaria-Neisser GE, Fish KM, Imachi M, Kuczkowski RL. J. Am. Chem. Soc. 1986; 108:3837–3838.
7. a) Estell DA, Graycar TP, Wells JA. J. Biol. Chem. 1985; 260:6518–6521. [PubMed: 3922976] b) Kim SJ, Joo JC, Song BK, Yoo YJ, Kim YH. Biotechnol. Bioeng. 2015; 112:668–676. [PubMed: 25335829] c) Dick M, Hartmann R, Weiergräber OH, Bisterfeld C, Classen T, Schwarten M, Neudecker P, Willbold D, Pietruszka J. Chem. Sci. 2016; 7:4492–4502.

8. Reactions with purified enzyme were observed to give lower activity and selectivity than reactions with whole cells, consistent with previous reports from this laboratory on whole-cell non-natural carbene and nitrene transfer reactions.

9. Wolf JR, Hamaker CG, Djukic J-P, Kodadek T, Woo LK. J. Am. Chem. Soc. 1995; 117:9194–9199.

10. a) Kent UM, Juschyshyn ML, Hollenberg PF. Curr. Drug. Metab. 2001; 2:215–243. [PubMed: 11513328] b) Hollenberg PF, Kent UM, Bumpus NN. Chem. Res. Toxicol. 2008; 21:189–205. [PubMed: 18052110] c) Hirao H, Cheong ZH, Wang X. J. Phys. Chem. B. 2012; 116:7787–7794. [PubMed: 22620991]

11. Komives EA, Tew D, Olmstead MM, Ortiz de Montellano PR. Inorg. Chem. 1988; 27:3112–3117.

12. Ortiz de Montellano PR, Kunze KL, Beilan HS, Wheeler C. Biochemistry. 1982; 21:1331–1339. [PubMed: 6122467]

13. Setsune J, Iida T, Kitao T. Tetrahedron Lett. 1988; 29:5677–5680.

14. a) Khade RL, Fan W, Ling Y, Yang L, Oldfield E, Zhang Y. Angew. Chem. Int. Ed. 2014; 53:7574–7578.b) Sharon DA, Mallick D, Wang B, Shaik S. J. Am. Chem. Soc. 2016; 138:9597–9610. [PubMed: 27347808]

15. Li H, Poulos TL. Nat. Struct. Biol. 1997; 4:140–146. [PubMed: 9033595]

16. Brustad EM, Lelyveld VS, Snow CD, Crook N, Jung ST, Martinez FM, Scholl TJ, Jasanoff A, Arnold FH. J. Mol. Biol. 2012; 422:245–262. [PubMed: 22659321]

17. McIntosh JA, Heel T, Buller AR, Chio L, Arnold FH. J. Am. Chem. Soc. 2015; 137:13861–13865. [PubMed: 26299431]

18. a) Whitehouse CJC, Bell SG, Wong L-L. Chem. Soc. Rev. 2012; 41:1218, 1260. [PubMed: 22008827] b) Jung ST, Lauchli R, Arnold FH. Curr. Opin. Biotechnol. 2011; 22:809–817. [PubMed: 21411308]

19. Sevrioukova I, Li H, Zhang H, Peterson JA, Poulos TL. Proc. Natl. Acad. Sci. USA. 1999; 96:1863–1868. [PubMed: 10051560]

20. Tran N-H, Nguyen D, Dwaraknath S, Mahadevan S, Chavez G, Nguyen A, Dao T, Mullen S, Nguyen T-A, Cheruzel LE. J. Am. Chem. Soc. 2013; 135:14484–14487. [PubMed: 24040992]

21. For example: Ganea A, Harding JJ. Eur. J. Biochem. 1995; 231:181–185. [PubMed: 7628468] Hook DWA, Harding JJ. FEBS Letters. 1996; 382:281–284. [PubMed: 8605985]

22. For example: Zimmerman SB, Pheiffer BH. Proc. Natl. Acad. Sci. USA. 1983; 80:5852–5856. [PubMed: 6351067] Guo Z-F, Jiang M, Zheng S, Guo Z. Bioorg. Med. Chem. Lett. 2010; 20:3855–3858. [PubMed: 20627563] Moran-Zorzano MT, Viale AM, Munoz FJ, Alonso-Casajus N, Eydallin GG, Zugasti B, Baroja-Fernandez E, Pozueta-Romero J. FEBS Letters. 2007; 581:1035–1040. [PubMed: 17306798]

23. a) Bunn HF, Jandl JH. Proc. Natl. Acad. Sci. USA. 1966; 56:974–978. [PubMed: 5230192] b) Bunn HF, Jandl JH. J. Biol. Chem. 1968; 243:465–475. [PubMed: 4966113] c) Hunter CL, Mauk AG, Douglas DJ. Biochemistry. 1997; 36:1018–1025. [PubMed: 9033391]

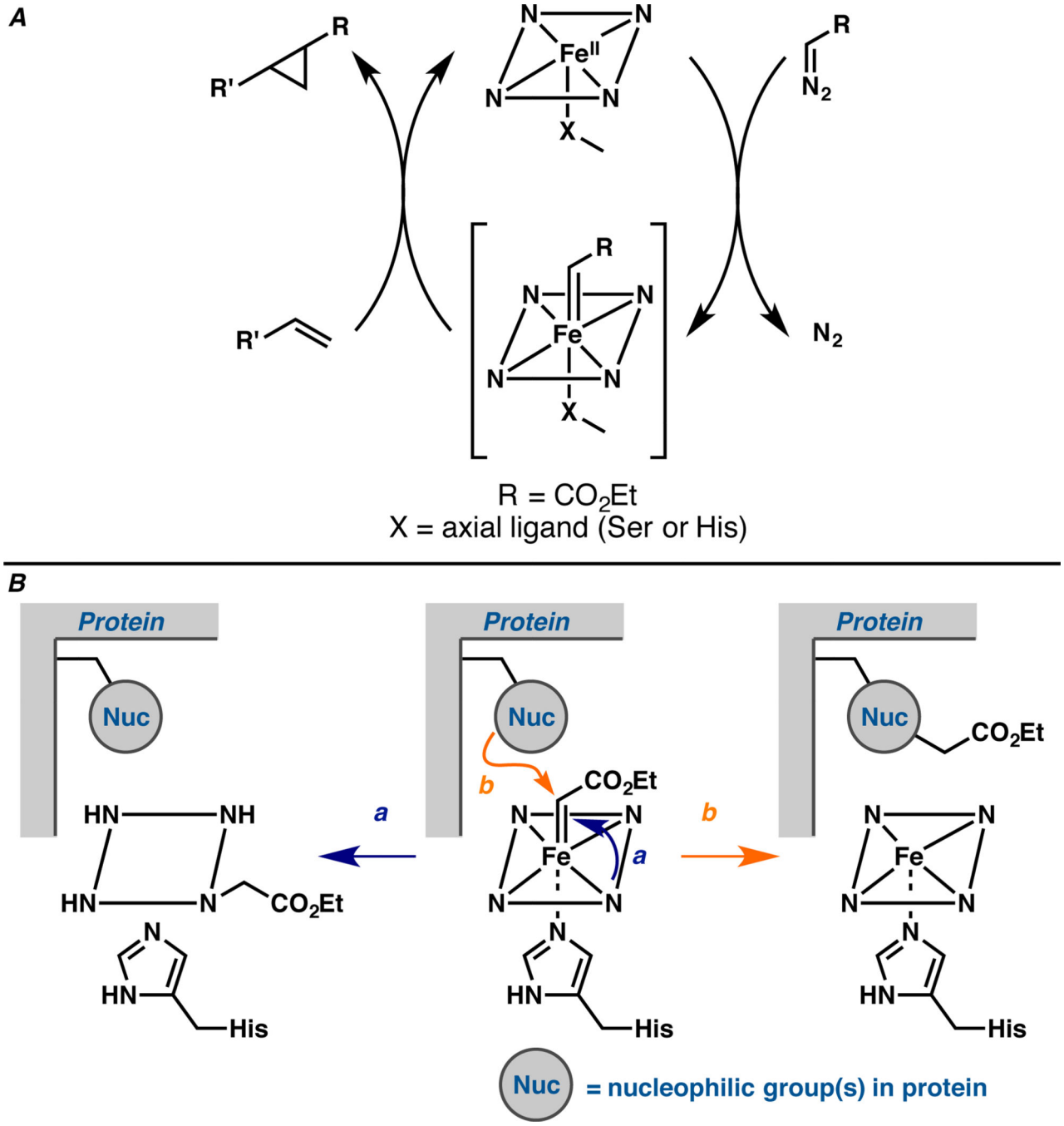

Figure 1.

A. Proposed catalytic cycle for heme protein-catalyzed carbene transfer to an olefin starts from the reduced ferrous state, which undergoes reaction with a diazo compound to form the putative iron carbenoid. The carbenoid reacts with an olefin, forming the cyclopropane product and regenerating the ferrous heme protein. **B.** Proposed mechanism-based inactivation via (a) porphyrin and (b) side chain modification involving the same iron carbenoid intermediate that mediates productive olefin cyclopropanation.

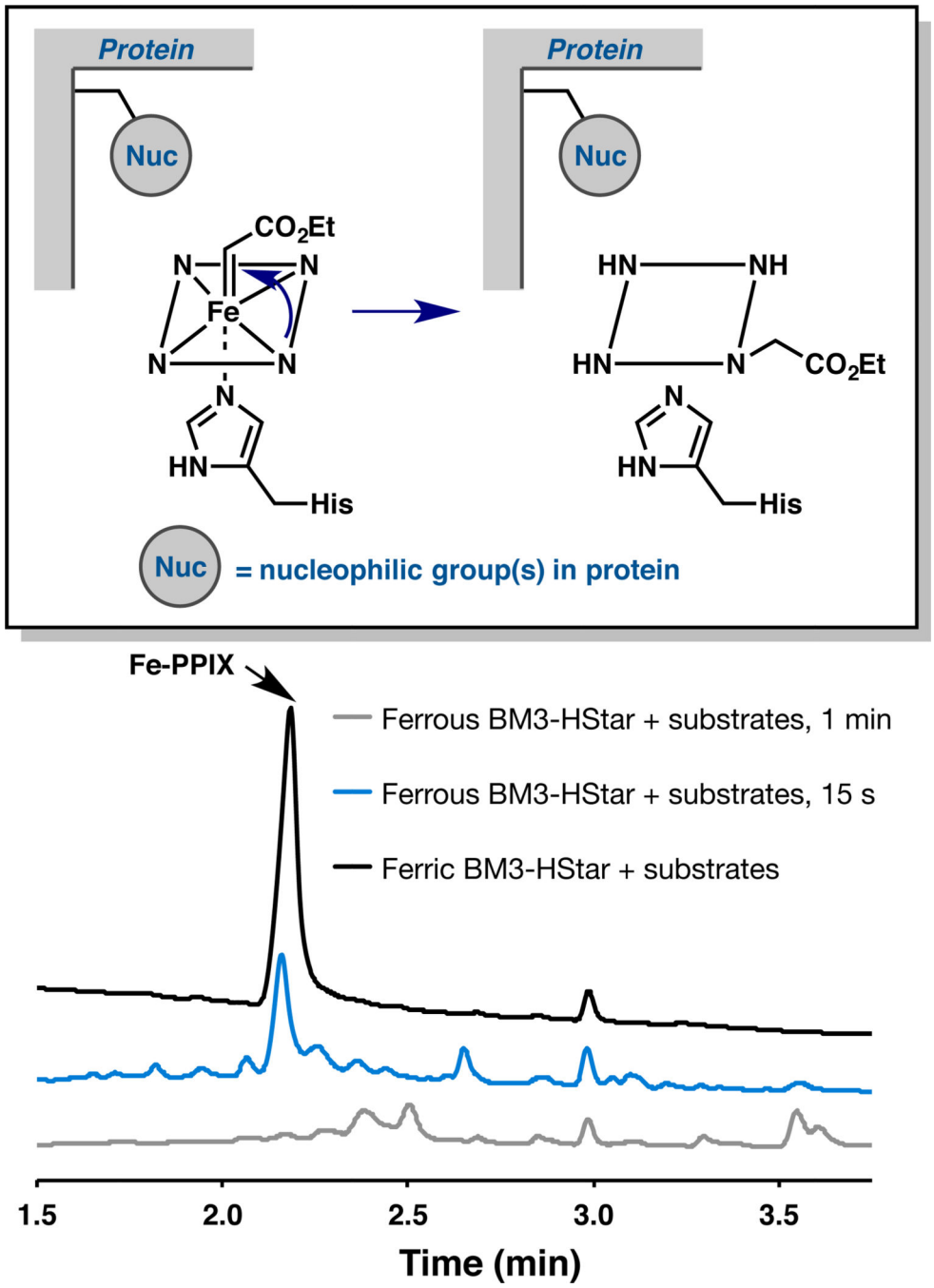

Figure 2.

LC-MS monitoring of heme content of the reaction mixture (MWD set at 330 nm) at different reaction times: amount of unmodified heme decreases during the course of the reaction, and new species appear.

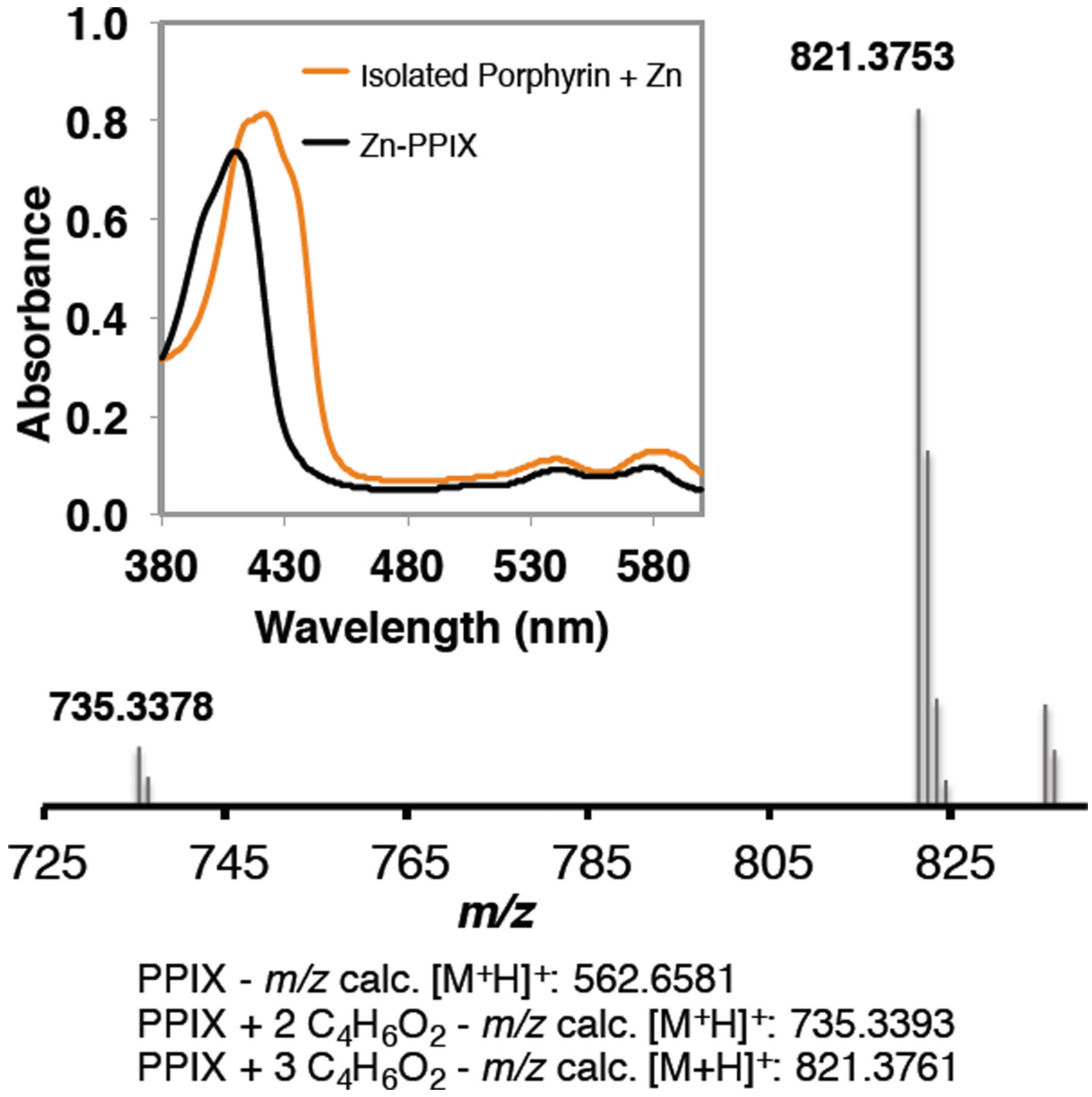

Figure 3.

Inset: Electronic absorption spectrum of porphyrin isolated after the cyclopropanation reaction as the Zn-complexed form indicates modification; spectrum of Zn-PPIX standard is provided for comparison. High-resolution mass spectrometry (HRMS) analysis of modified porphyrin isolated after the cyclopropanation reaction, showing major peaks with m/z of 735.3378 and 821.3753, which correspond to multiple additions of $C_4H_6O_2$ fragment.

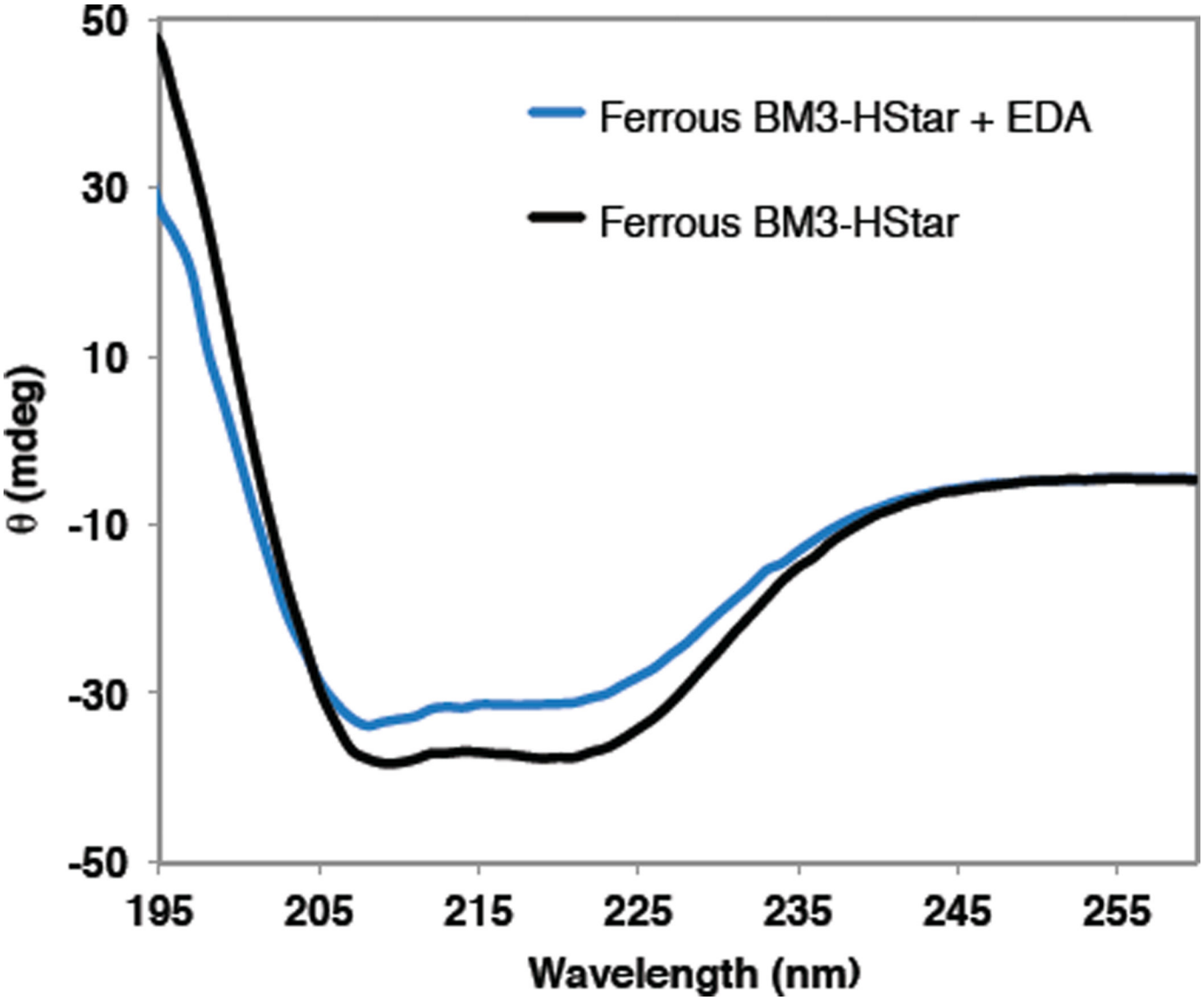

Figure 4.

Circular dichroism (CD) spectra of ferrous BM3-HStar before (black) and after reaction with EDA (blue). Decrease in molar ellipticity at 222 nm suggests a change in the secondary structure after the reaction, specifically a decrease in α-helical content and an increase in random coil.

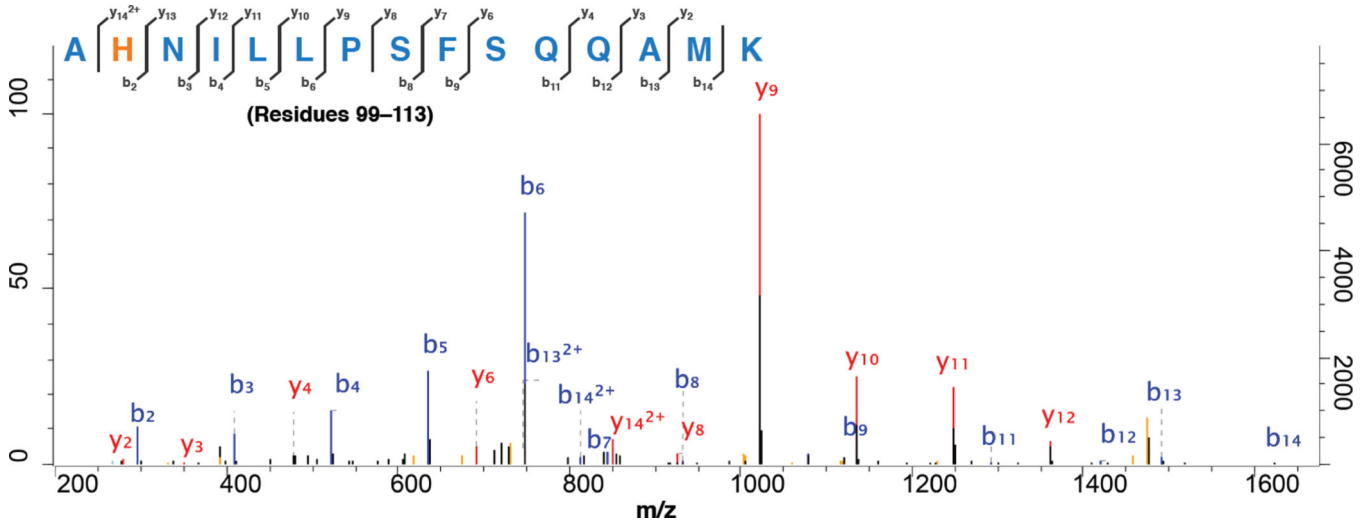

Figure 5.

Representative LC-MS/MS analysis of peptide fragments from crude cyclopropanation mixture. Modified peptides from inactivated BM3-HStar were analyzed using mass spectrometry after incubation with $Na_2S_2O_4$, EDA and **1** for 5 s. The modified residue is highlighted in orange. For complete LC-MS/MS traces of peptide fragments from the reaction mixture, see Figure S6 (Supplementary Information).

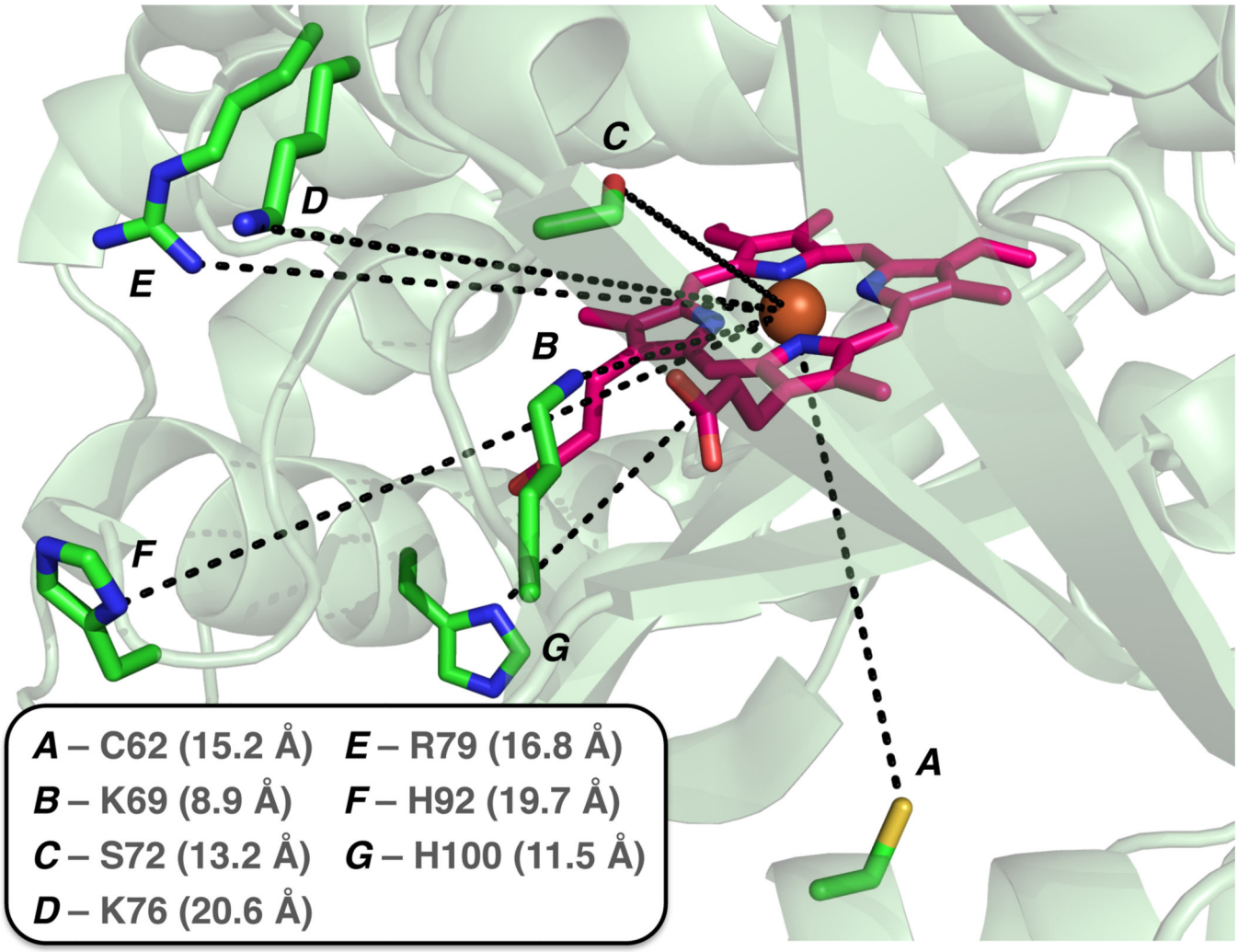

Figure 6.

Location of alkylated residues relative to the heme cofactor as mapped onto WT BM3 crystal structure (PDB ID: 2IJ2). Measured distances to the Fe center (in parentheses) are determined based on the WT BM3 crystal structure.

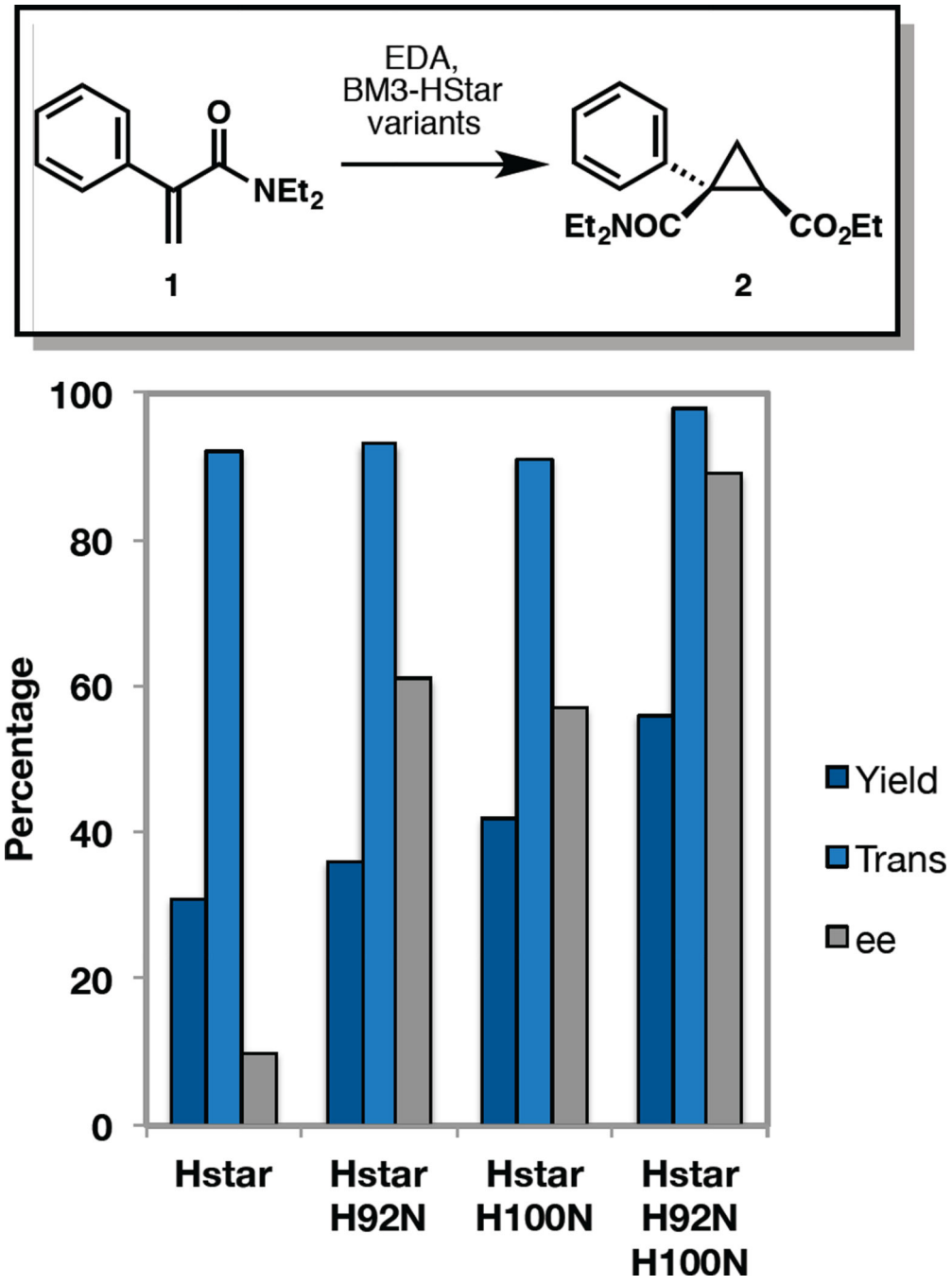

Figure 7.

Site-directed mutagenesis of BM3-HStar to improve yield and selectivity of cyclopropanation of acrylamide **1** with EDA. Reactions were performed with 10 μM enzyme, 10 mM of **1**, 20 mM of EDA, and 10 mM of $Na_2S_2O_4$ in 100 mM KPi buffer (pH = 8.0). Yields and diastereoselectivity were determined by GC calibrated for **2**. Enantioselectivity was determined by chiral SFC (See Supporting Information for GC yield determination).

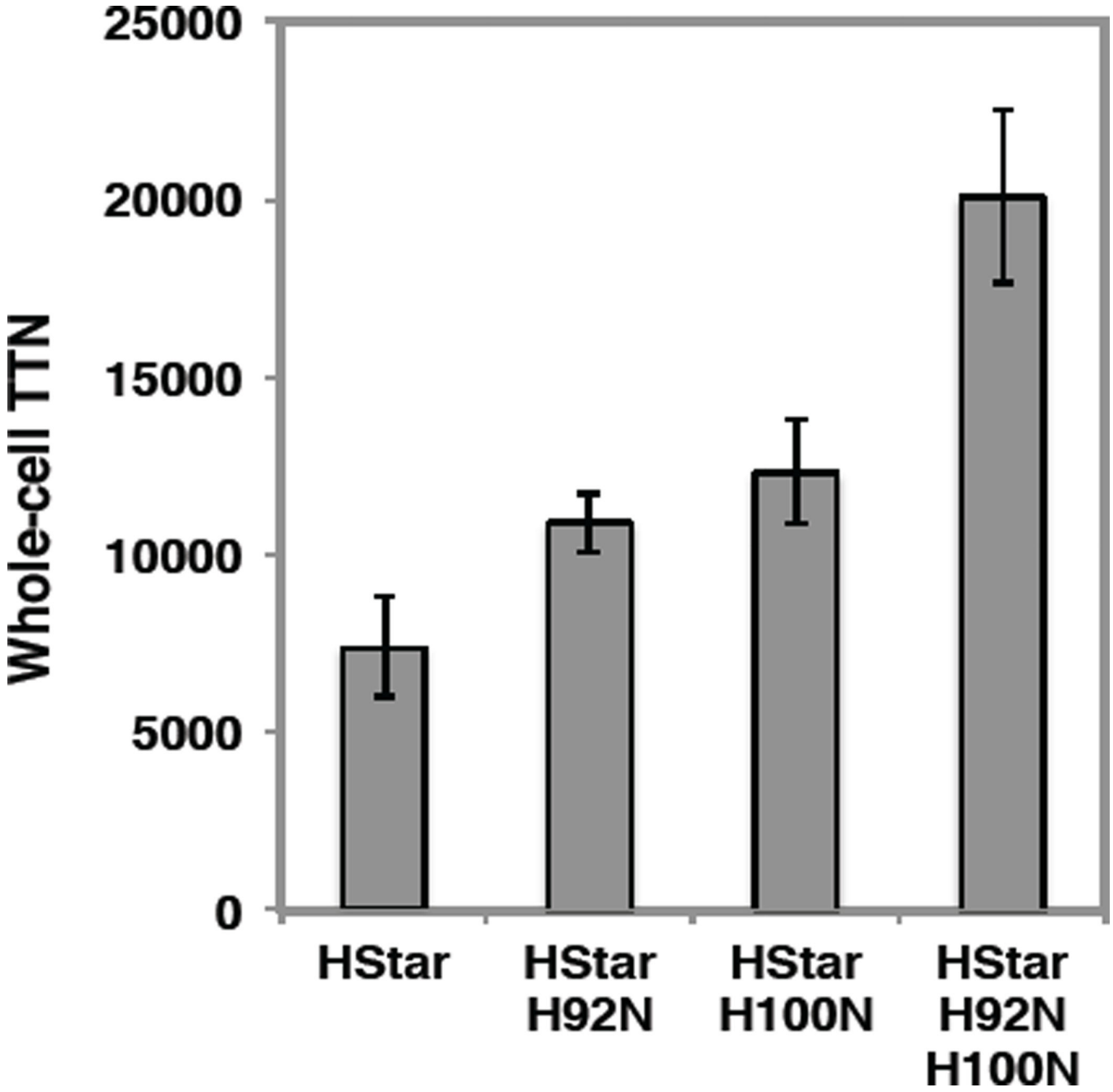

Figure 8.

Total turnover numbers (TTNs) for cyclopropanation of **1** with whole cells expressing BM3-HStar variants. Reactions were performed with whole cells expressing the enzyme (resuspended in M9-N media to OD600 = 10), 10 mM of **1**, and 20 mM of EDA. TTN = [product]/[enzyme]; enzyme concentration in whole-cell suspension was determined by ferrous expression assay (See Supporting Information for assay procedure); product concentration at the end of the reaction was determined by GC calibrated for **2**.

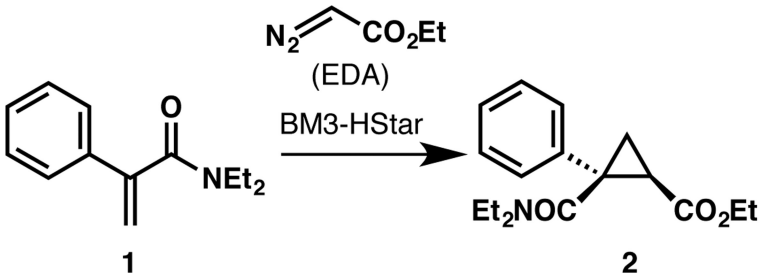

whole-cell cyclopropanation at OD_{600} = 60

1 (mM)	EDA (mM)	yield (%)	ee (%)
10	20	92	92
20	40	65	86
50	100	28	50
150	300	10	0

Scheme 1.

Observed erosion in yield and enantioselectivity of cyclopropanation with BM3-HStar in whole *E. coli* cells at high substrate concentrations.